

Tunable Bi-frustrated Electron Spin and Charge States in a Cu-Hexaaminobenzene Framework

Wei Jiang^a, Zheng Liu^{b,1}, Jia-Wei Mei^{c,a,1}, Bin Cui^{d,a}, and Feng Liu^{e,a,1}

^aDepartment of Materials Science and Engineering, University of Utah, Salt Lake City, UT 84112, USA; ^bInstitute for Advanced Study, Tsinghua University, Beijing 100084, China; ^cInstitute for Quantum Science and Engineering, and Department of Physics, Southern University of Science and Technology, Shenzhen 518055, China; ^dSchool of Physics, Shandong University, Jinan 250100, China; ^eCollaborative Innovation Center of Quantum Matter, Beijing 100084, China

This manuscript was compiled on August 6, 2021

A geometrically frustrated lattice may host frustrated electron spin or charge states that spawn exotic quantum phases. We show that a newly synthesized metal-organic framework of Cu-Hexaaminobenzene [Cu₃(HAB)₂] exhibits a multi spectra of unusual quantum phases long sought after in condensed matter physics. On one hand, the Cu²⁺ ions form an ideal *S*-1/2 antiferromagnetic kagome lattice. On the other hand, the conjugated-electrons from the organic ligands give rise to completely dispersionless energy bands around the Fermi level, reproducing a frustrated π_x - π_y hopping model on a honeycomb lattice. We propose to characterize the coexistence of frustrated local spins and conjugated electrons through scanning tunneling microscopy simulations. Most remarkably, their close energy proximity enables one to tune the system between the two frustrated states by doping up to one hole per HAB unit. Thus, Cu₃(HAB)₂ provides a unique exciting platform to investigate the interplay of frustrated spins and electrons in one single lattice, e.g. by gating experiments, which will undoubtedly raise interesting theoretical questions leading to possible new condensed-matter phases.

Quantum spin liquid | flat band | strongly-correlated system | metal-organic framework

Development in modern chemical synthesis is turning metal-organic frameworks (MOF) into a playful legoland for condensed matter physicists, where lattice structures with desired electronic and magnetic properties can be delicately tailored with diverse metal ions and organic linkers (1–4). The most recent fascination is about the “frustrated” spins or electrons triggered by special lattice geometry. The frustration is considered to suppress classical orders and lead to highly nontrivial quantum-entangled phases, such as quantum spin liquid (QSL) state (5–7). Experiments in inorganic systems, namely herbertsmithite (8–10) and Zn-barlowite (11), suggest a gapped QSL in a kagome spin system although the existence of the gap is still under debate (12–18). Several organic molecular crystals are among the most promising QSL candidates (19–23), e.g. κ -(BEDT-TTF)₂Cu₂(CN)₃ and EtMe₃Sb[Pd(dmit)₂]₂, both of which are found to have a charge insulating yet spin fluctuating ground state. Very recently, it was proposed that Kitaev spin liquid could be realized in a MOF with Ru³⁺ (24).

There are also first-principles MOF designs of “frustrated metal”. For example, in an In-phenylene framework (25), calculation predicts completely dispersionless electronic bands around the Fermi level. The underlying physics is described by a frustrated p_x - p_y hopping model on a honeycomb lattice, which was previously mainly studied in cold-atom setups (26, 27). Because the kinetic energy is largely quenched, the dispersionless band, or “flat band”, naturally becomes an

interaction-dominated platform, giving rise to various instabilities, such as charge-density wave, ferromagnetism, superconductivity and even high-temperature fractional quantum Hall states (28–31).

Here, we discover a rare example, i.e. a Cu-hexaaminobenzene framework [Cu₃(HAB)₂, Cu₃(C₆N₆H₆)₂], that simultaneously hosts both frustrated spins and frustrated electrons. The crystalline Cu₃(HAB)₂ has already been synthesized by coordinating hexaaminobenzene (HAB) ligands and Cu ions through air-liquid or liquid-liquid interfacial interaction (32). As schematically shown in Fig. 1(a), the HAB ligands connect Cu ions into a two-dimensional (2D) periodic lattice; each Cu ion locally coordinates with four N atoms in a distorted planar square geometry. We reveal that this material can be viewed as a combination of two subsystems [Fig. 1(b)]. One is a kagome antiferromagnetic *S* = 1/2 lattice (KAFM) consisting of the Cu²⁺ ions. KAFM is considered as one of the most promising systems to realize QSL (33). The most fascinating feature in KAFM is the possible existence of fractional spinon excitations, which was speculated in theory decades ago and has been recently observed in experiments (9, 11). The other subsystem consists of $p_{x,y}$ -like ($\pi_{x,y}$) molecular orbitals on a honeycomb lattice, which give rise to an itinerant flat band right at the Fermi level. Because the flat band is susceptible to various spontaneous symmetry breaking, electrons in this band are considered to be in a fragile Fermi liquid (FL) state. Remarkably, the two subsystems are strongly coupled

Significance Statement

Both electron spin and charge can get frustrated in a geometrically frustrated lattice. If spins are favored to align antiferromagnetic in up and down direction on neighboring sites, they will be frustrated in a triangle lattice; if electrons move too slow in a lattice with a narrow bandwidth of quenched kinetic energy, they are in a frustrated charge state incapable of hopping independently because of Coulomb repulsion. Such frustrations leading to exotic quantum phases have fascinated theorists for a long time. However, real materials with frustrated spin lattice have only been identified recently. Here, we discover that a newly synthesized metal-organic framework [Cu₃(C₆N₆H₆)₂] hosts simultaneously both frustrated spins and electrons, affording an exciting platform to explore new exotic quantum phases.

W.J., Z.L., J.-W.M., and F.L. designed research; W.J. and J.-W.M. performed research; B.C. contributed new analytic tools; W.J., Z.L., J.-W.M., and F.L. wrote the paper.

The authors declare no conflict of interest.

¹To whom correspondence should be addressed. E-mail: fliu@eng.utah.edu, meijw@sustc.edu.cn, zheng-liu@mail.tsinghua.edu.cn.

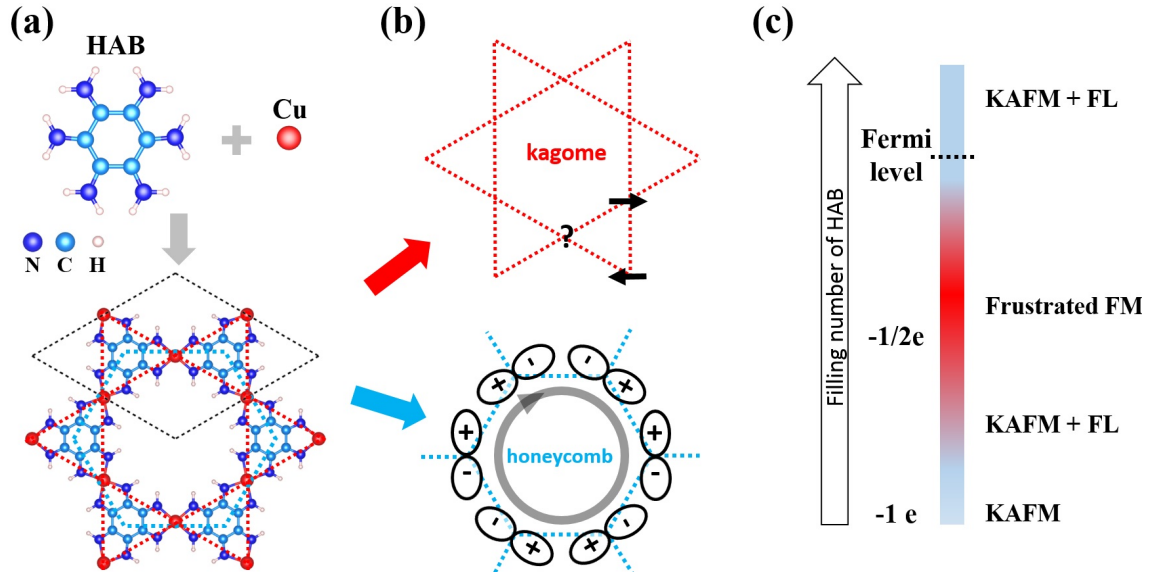


Fig. 1. Structural and electronic properties of $\text{Cu}_3(\text{HAB})_2$. (a) Atomic structure of a HAB molecule and the crystalline structure of $\text{Cu}_3(\text{HAB})_2$ by coordinating HAB with Cu. (b) Schematics of bifrustration in this material. (c) Phase evolution as a function of electron filling number of HAB.

within a close energy proximity, leading to the possibility of new phases with different amount of doping, which is experimentally feasible. The system can be readily tuned, e.g. by gating experiments into a series of quantum states with different electron filling, as illustrated in Fig. 1(c). The evolution of these quantum states will be discussed qualitatively before the end of this Article. The coupling between these two subsystems poses an important but difficult theoretical question, and a complete answer may strongly rely on new experimental input. The primary goal of the present work is to computationally substantiate the proposed bifrustration in this real material, and to establish a basis for future investigation.

Calculation results

We first calculated the band structure within the standard density functional theory (DFT, Supporting Information) [Fig. 2(a)]. Below the Fermi level (from -1.75 to -0.5 eV), there is a pair of isolated π_z Dirac bands just like the p_z -bands in graphene. Around the Fermi level (from -0.25 to 0.5 eV), there are seven bands, among which three are completely dispersionless, manifesting typical features of frustration. More importantly, the Fermi level almost coincides with one of the flat band. By resolving these bands according to the atomic composition, they can be decomposed into a three-band set (red) and a four-band set (blue). The three-band set mainly arises from the Cu ions, which can be nicely fitted by a single-orbital tight-binding (TB) hopping model on a kagome lattice [Fig. 2(b)]:

$$H_d^0 = t_d \sum_{\langle ij \rangle} (d_{i\sigma}^\dagger d_{j\sigma} + \text{H.c.}) \quad [1]$$

where the summation $\langle ij \rangle$ are constrained within the nearest-neighbors (NN) on the Cu kagome lattice indexed by i, j , and $t_d = 0.06$ eV is the fitted NN hopping amplitude. The four-band set arises from a combination of N and C orbitals, which reflects the typical features of an effective π_{xy} σ -bond hopping

model on a honeycomb lattice:

$$H_\pi^0 = t_\pi \sum_{\langle IJ \rangle} (\pi_I^\dagger \pi_J + \text{H.c.}) \quad [2]$$

where the summation $\langle IJ \rangle$ are constrained within the NN bonds on the HAB honeycomb lattice indexed by I, J . $\pi^{I\dagger}$ creates a superposition state of π_x and π_y orbitals with the orbital vector parallel to the bond, i.e. $|\pi^I\rangle = \cos\phi|\pi_x\rangle + \sin\phi|\pi_y\rangle$ with ϕ as the angle between the bond and the x -axis. $\pi_{x,y}$ are molecular conjugated orbitals from HAB with analogical symmetries to $p_{x,y}$ orbitals in single C or N atom. According to Fig. 3(a), they distribute among both C and N atoms. In this model, t_π is equivalent to the σ -bond hopping amplitude, while the weak π -bond hopping is neglected. The fitted value for t_π is 0.22 eV [Fig. 2(c)]. We noticed that the LDA band structure could be better reproduced by further considering that the π^I -orbitals on the NN sites have a small overlap $S = \langle \pi_I^\dagger | \pi_J \rangle = 0.18$. The generalized eigenvalue problem becomes $\det(H_\pi^0 - \epsilon S) = 0$, where ϵ is the eigenenergy.

To fully characterize this intriguing material beyond DFT, two additional questions should be answered: (a) What is the basis of these hopping models? The nonorthogonality of the effective $\pi_{x,y}$ -orbitals revealed from the band fitting already implies that they should be complicated molecular orbitals; (b) How does interaction change the picture? This question is particularly important to the kagome bands arising from Cu, because Cu $3d$ -electrons are known to experience strong Coulomb repulsion.

These questions can be partially addressed by studying the building blocks of $\text{Cu}_3(\text{HAB})_2$ based on the state-of-the-art quantum chemistry computational package (Gaussian). We proceed by a ‘‘computational thought experiment’’ to first analyze a single HAB molecule [Fig. 3(a)] and then sandwich one Cu atom between two HAB molecules [Fig. 3(b)]. Figure 3(c) shows the three highest occupied levels of a single HAB molecule. We also plot the wavefunction of these three levels. It is clear that they mainly arise from the π -conjugation

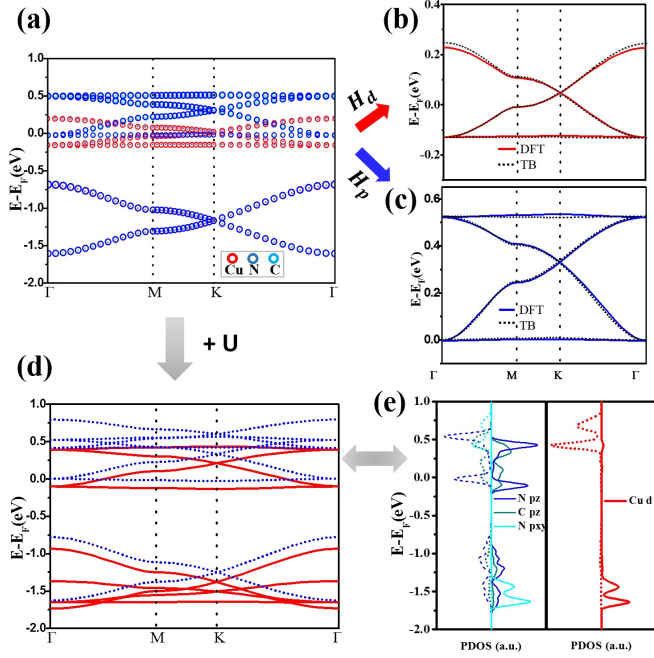


Fig. 2. Band structures from DFT, DFT+U and the effective TB models. (a) Atomic-resolved DFT band structure; the marker size indicates the weight of the atomic composition. Decomposition of the bands into (b) a kagome lattice and (c) a honeycomb lattice, with comparison to the effective TB model band structure. (d) The DFT+U band structure; the solid (red) and dashed (blue) curves corresponds to different spins. (e) The DFT+U projected density of states.

of the C/N p_z -orbitals. The two degenerate levels π_x and π_y on top have the same symmetry as the atomic p_x and p_y orbitals. The single level below π_z has the same symmetry as the atomic p_z orbital. The molecular $\pi_{x,y}$ -orbitals define the basis of Eq. 2. In a single molecule, $\pi_{x,y,z}$ are all fully occupied.

Figure 3(d) shows the evolution of the occupied levels after putting a Cu atom between two HAB molecules. The highest occupied level now becomes a half-filled single orbital primarily consisting of the Cu 3d orbital. By choosing the Cu-N bonds as the orbital quantization axes, this molecular orbital is equivalent to an atomic $d_{x^2-y^2}$ -orbital. All the other Cu 3d-orbitals are found to be deep down away from the Fermi level and fully occupied. Hence, Cu is in a +2 ($3d^9$) valence state, or equivalently, contains one single hole. The situation is actually very similar to that in high- T_c cuprate superconductors(34), where the Cu-O planar crystal field splits out a half-filled $d_{x^2-y^2}$ -orbital, and the dynamics of this dangling bond is the microscopic origin of all the unusual electronic properties(34). The $\pi_{x,y}$ orbitals now become the second highest occupied levels. They are still degenerate, but the filling factor reduces from 1 to $\frac{3}{4}$. This result can be understood by noticing that to bond with Cu, the two HAB molecules release four H^+ ions in total. The Cu^{2+} ion, however, can only donate two electrons to the HAB molecules. Consequently, upon bonding with a Cu, each HAB molecule loses one out of its four $\bar{p}_{x,y}$ electrons.

We can now re-evaluate the DFT results. The effective four-band model on a honeycomb lattice (Eq. 2) can be firmly constructed out of the $\pi_{x,y}$ orbitals. These orbitals are itinerant, and thus should be well captured by DFT. The filling factor of the four-band set should be $\frac{1}{4}$, considering that

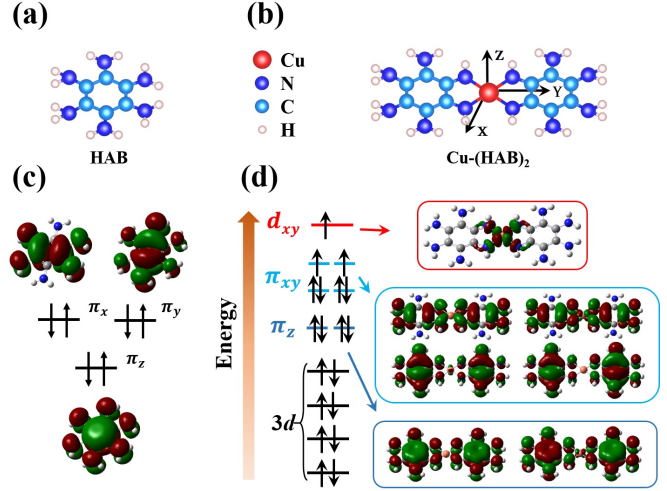


Fig. 3. Energy levels and the associated wavefunction of (a) a HAB molecule and (b) a $Cu-(HAB)_2$ cluster

each HAB ligand bonds with three Cu ions in the periodic $Cu_3(HAB)_2$ framework (Supporting Information). This means that the bottom flat band is fully occupied and all the other three bands are empty. The location of the Fermi level calculated from LDA correctly captures this property. The origin of the flat band lies in a special localized eigenstate as sketched in Fig. 1(b). Electrons in this eigenstate cannot leak outside the hexagon due to complete destructive interference (26).

With respect to the kagome degree of freedom, the $Cu-(HAB)_2$ cluster calculation indicates that each Cu^{2+} ion contains a local spin, whereas the DFT calculation suggests the formation of a nonmagnetic metal with the Fermi level crossing the half-filling energy. This is the widely known failure of DFT due to the underestimation of electron correlation. A simple remedy within the DFT formalism is to include electron correlations in a Hartree-Fock mean-field manner, know as the +U correction. It has been demonstrated that DFT+U can correctly reproduce Mott insulating gap by explicitly breaking the time-reversal symmetry. Figure 2(d) shows the resulted band structure by choosing the empirically averaged Coulomb interaction $\bar{U} \sim 5$ eV as commonly used for Cu. By referring to the projected density of states (PDOS) [Fig. 2(e)], we found that the Cu kagome band is split into a set of lower Hubbard bands and a set of upper Hubbard bands. The Mott gap (U_0) is about 2 eV, much smaller than $\bar{U} \sim 5$ eV. It reflects the strength of onsite Coulomb repulsion in the presence of Coulomb screening due to itinerant conjugated π -electrons in the system. The complete Hamiltonian for this Cu^{2+} degree of freedom can then be revised into:

$$H_d = H_d^0 + U_0 \sum_I n_{i\uparrow} n_{i\downarrow}. \quad [3]$$

The hopping amplitude $t_d = 0.06$ eV in H_d^0 is much smaller than U_0 . Therefore, at half filling, the large- U perturbation can be applied, which maps H_d into a $S=1/2$ Heisenberg model:

$$H_d \simeq J_d \sum_{\langle ij \rangle} \mathbf{S}_i \cdot \mathbf{S}_j, \quad [4]$$

where $J_d = \frac{4t_d^2}{U_0} \simeq 7$ meV is the strength of the AFM NN spin exchange. This AFM superexchange strength is small because

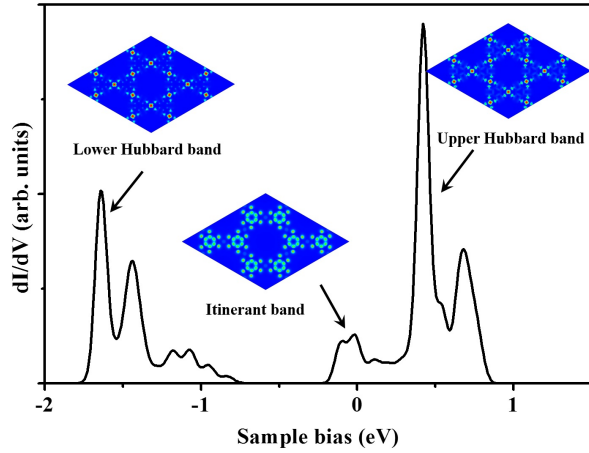


Fig. 4. STM simulations. Main figure displays the dI/dV spectra simulated for $\text{Cu}_3(\text{HAB})_2$ surface, showing two prominent Hubbard peaks below and above the Fermi level along with one itinerant peak at the Fermi level. The insets show the STM topography of $\text{Cu}_3(\text{HAB})_2$ surface with bias of 0.45/-1.55 and 0 eV corresponding to the kagome upper/lower Hubbard and honeycomb itinerant band, respectively.

of the large distance between Cu^{2+} ions. Furthermore, the $\pi_{x,y,z}$ molecular orbitals around the Fermi level primarily arise from the C/N atomic p_z orbitals, which are orthogonal to the $d_{x^2-y^2}$ -orbital. Thus, there is no charge transfer between $\pi_{x,y}$ orbitals on HAB ligands and $d_{x^2-y^2}$ -orbital on Cu ions (Supporting Information). For the same reason, the superexchange for Cu $3d$ orbitals is scaled by on-site Coulomb interaction U_0 .

One more important point revealed in Fig. 2(d) is that a Zeeman splitting of the π_{xyz} bands occurs. This splitting is not related to the instability of the π_{xy} flat band, because the π_z Dirac bands are also split of the same amount. Therefore, it should be attributed to the coupling with the Cu local spin. It is clear from Fig. 2(e) that the downshifted (upshifted) π_{xyz} bands have the same (opposite) spin direction as the Cu spin, indicating a ferromagnetic (FM) Hund's coupling:

$$H_{\pi d} = -J_H \sum_i \sum_{I \in \text{NN}(i)} \mathbf{S}_i \cdot \mathbf{s}_I, \quad [5]$$

where \mathbf{S}_i and $\mathbf{s}_I = \sum_{\alpha=x,y} \sum_{\sigma=\uparrow/\downarrow} \sigma \pi_{I\alpha\sigma}^\dagger \pi_{I\alpha\sigma}$ are the spin operators of the Cu $d_{x^2-y^2}$ electron and the NN HAB π_{xy} electrons, respectively. J_H denotes the Hund's coupling strength, which is roughly of the same magnitude as the Zeeman splitting ~ 0.1 eV.

To directly identify these two frustrated degrees of freedom, we propose to carry out scanning tunneling microscopy (STM) measurement of this material. STM has been widely applied to study the self-assembled metal-organic coordinated systems built through intermolecular hydrogen, covalent and coordinate bonding (35, 36). Among those studies, many 2D network structures have been successfully synthesized through coordination bond between Cu and N atoms on various substrates (37–39), which makes growing and studying monolayer $\text{Cu}_3(\text{HAB})_2$ through STM feasible and promising. Thus, we have simulated scanning tunneling spectroscopy (STS) mapping at two characteristic regions, as demonstrated in Fig. 4. The dI/dV spectra shows two prominent Hubbard peaks below and above the Fermi level along with itinerant peaks right on the Fermi level. The STM topography simulations around the upper/lower Hubbard peak with a bias of 0.45/-1.55 eV

exhibit clear kagome patterns, and a honeycomb feature is observed for the bias of 0 eV around the itinerant peaks, as shown in the insets of Fig. 4. It is worth mentioning that our STM results are simulated for insulating substrates, where all the states will remain intact in the insulating gap.

Discussion

By combining the results above, we arrive at a full effective hamiltonian characterizing this unique material:

$$H = H_\pi^0 + H_d + H_{\pi d}, \quad [6]$$

which appears like a typical spin-fermion model as employed for iron pnictide high-temperature superconductors(40–42) and colossal magnetoresistance manganites (43, 44). The interplay between the conducting electrons and local spins also lead to ubiquitous physical phenomena in other systems, such as the Kondo problems (45, 46), the heavy fermion systems (47, 48), cuprate high temperature superconductors (34, 49, 50). The situation of $\text{Cu}_3(\text{HAB})_2$ is actually even more exotic - beyond the dichotomy between electron localization and itinerancy, as the spin and fermion also simultaneously suffer from strong frustration.

This bifrustrated spin-fermion model presents a new theoretical problem that remains to be explored by strong-correlation calculation methods, such as density matrix renormalization group (51). On the other hand, the electron filling of the HAB ligands can be delicately tuned through either gating or chemical redox control (52, 53), which will result in various interesting quantum states.

Here, we will give some preliminary discussions about the phase evolution of $\text{Cu}_3(\text{HAB})_2$ with different doping concentration, based on the existing knowledge of the subsystems. When all the π electrons are removed (1e per HAB ligand, $1.24 \times 10^{14} \text{ cm}^{-2}$), the system is at the H_d side of the KAFM state, which is a hot topic in condensed matter physics in the past decade (33). It is generally believed that H_d alone will give rise to QSL with fractional spinon excitations. After adding H_π^0 by doping small amount of π electrons, one simple possibility is that these fractional spinons can peacefully coexist with frustrated fermions in some circumstances, forming together a “fractional Fermi liquid” (FL*)(48, 54).

When considering only the H_p^0 system without H_d , there is a rigorous theorem originally proved by Mielke (55, 56), known as “flat-band ferromagnetism”. It states that when an on-site Coulomb repulsion of any finite magnitude is turned on, the half-filled flat band has a fully-polarized FM ground state. It was later demonstrated that the flat-band ferromagnetism is stable against small perturbations. In some sense, the flat-band ferromagnetism represents the large-DOS limit of Stoner's criteria, complimentary to Nagaoka's ferromagnetism under the large-U limit.

Thus, with more π electrons doped into the system, the flat-band ferromagnetism occurs and the itinerant fermions will act as a strong magnetic field on the spins via $H_{\pi d}$. Recall that the Hund's coupling J_H is of the order of 100 meV, much larger than the AFM superexchange $J_d \simeq 7$ meV between spins. Consequently, the KAFM subsystem is also polarized into a FM configuration. Indeed, within the DFT+U formalism, we find that if we manually tunes the Fermi level to the half-filling point, which corresponds to extract 1/2 electron from each HAB on average, the spin degeneracy of the flat band is

spontaneously lifted, and the FM Cu spin order has the lowest energy (Supporting Information).

It is straightforward to perform a spin-wave expansion on Eq. 3 with respect to the FM polarized ground state: $S_i^{\dagger} = b_i$, $S_i^{-1} = b_i^{\dagger}$, $S_i^z = \frac{1}{2} - b_i^{\dagger}b_i$, in which b corresponds to the Holstein-Primakoff boson, or magnon annihilation operator. Replacing the spin operators in Eq. (3) with b^{\dagger} and b , H_d is transformed into:

$$H_d = \frac{J_d}{2} \sum_{\langle ij \rangle} (b_{i\sigma}^{\dagger} b_{j\sigma} + \text{H.c.}) + \text{const.} \quad [7]$$

This Hamiltonian appears almost the same as Eq. (1). The main difference is that the hopping particle transforms from a fermionic electron to a bosonic magnon. Obviously, the magnon band structure is the same as Fig. 2(b) after rescaling them with energy. It is important to note that the flat band is carried over to the magnon degree of freedom. The FM ground state is thus susceptible to various instabilities. In Fig. 1(c), we label this regime as a “frustrated ferromagnet (FM)”.

Conclusion and perspective

In conclusion, we have numerically demonstrated the coexistence of frustrated local spins and frustrated itinerant electrons in $\text{Cu}_3(\text{HAB})_2$. Each of these two frustrated degrees of freedom is known to produce a rich phase diagram alone, and we argue that a real platform that simultaneously contains both will open even more possibilities. An effective model is constructed, but the theoretical solution has to rely on sophisticated numerical computations. Further experimental input is highly demanded, especially, the close energy proximity of the frustrated spin bands and charge bands enables a high tunability by gating to study the interplay between different quantum phases. One great challenge is to further improve the $\text{Cu}_3(\text{HAB})_2$ crystalline quality. We have simulated the scanning tunneling spectroscopy and real-space mapping under different bias, which can be used to resolve the two types of frustrated lattices. The redox control techniques may also provide an alternate doping method to modify the electron filling of $\text{Cu}_3(\text{HAB})_2$ lattice.

Materials and Methods

The crystal properties were calculated using first-principles methods based on density functional theory with Vienna *ab initio* simulation package code. The molecular properties of HAB molecule and $\text{Cu}-(\text{HAB})_2$ complex were calculated using Gaussian package with the B3LYP functional. More details are presented in [Supporting Information](#).

ACKNOWLEDGMENTS. J.-W. Mei and F. Liu are supported by U.S. DOE-BES (Grant No. DE-FG02-04ER46148). W. J. is supported by the National Science Foundation-Material Research Science & Engineering Center (NSF-MRSEC grand No. DMR-1121252). Z. L. is supported by NSFC under Grant No. 11774196. We thank the CHPC at the University of Utah and DOE-NERSC for providing the computing resources.

- Lu W, et al. (2014) Tuning the structure and function of metal-organic frameworks via linker design. *Chem. Soc. Rev.* 43(16):5561–5593.
- Deria P, et al. (2014) Beyond post-synthesis modification: evolution of metal-organic frameworks via building block replacement. *Chem. Soc. Rev.* 43(16):5896–5912.
- Brozek CK, Dinca M (2014) Cation exchange at the secondary building units of metal-organic frameworks. *Chem. Soc. Rev.* 43(16):5456–5467.
- Colon YJ, Snurr RQ (2014) High-throughput computational screening of metal-organic frameworks. *Chem. Soc. Rev.* 43(16):5735–5749.

- Anderson PW (1987) The resonating valence bond state in La_2CuO_4 and superconductivity. *Science* 235(4793):1196.
- Lee PA (2008) An End to the Drought of Quantum Spin Liquids. *Science* 321(5894):1306–1307.
- Balents L (2010) Spin liquids in frustrated magnets. *Nature* 464(7286):199–208.
- Shores MP, Nytko EA, Bartlett BM, Nocera DG (2005) A structurally perfect $S = 1/2$ kagome antiferromagnet. *J. Am. Chem. Soc.* 127(39):13462–13463.
- Han TH, et al. (2012) Fractionalized excitations in the spin-liquid state of a kagome-lattice antiferromagnet. *Nature* 492(7429):406–410.
- Fu M, Imai T, Han TH, Lee YS (2015) Evidence for a gapped spin-liquid ground state in a kagome Heisenberg antiferromagnet. *Science* 350(6261):655–658.
- Feng Z, et al. (2017) Gapped spin-1/2 spinon excitations in a new kagome quantum spin liquid compound $\text{Cu}_3\text{Zn}(\text{OH})_6\text{F}_6$. *Chinese Physics Letters* 34(7):077502.
- Yan S, Huse DA, White SR (2011) Spin-liquid ground state of the $s = 1/2$ kagome heisenberg antiferromagnet. *Science* 332(6034):1173–1176.
- Depenbrock S, McCulloch IP, Schollwöck U (2012) Nature of the spin-liquid ground state of the $s = 1/2$ heisenberg model on the kagome lattice. *Phys. Rev. Lett.* 109(6):067201.
- Jiang HC, Wang Z, Balents L (2012) Identifying topological order by entanglement entropy. *Nat Phys* 8(12):902–905.
- Mei JW, Chen JY, He H, Wen XG (2017) Gapped spin liquid with F_2 topological order for the kagome heisenberg model. *Phys. Rev. B* 95(23):235107.
- He YC, Zaleel MP, Oshikawa M, Pollmann F (2016) Signatures of dirac cones in a dmrg study of the kagome heisenberg model. *arXiv preprint arXiv:1611.06238*.
- Jiang S, Kim P, Han JH, Ran Y (2016) Competing spin liquid phases in the $s=1/2$ heisenberg model on the kagome lattice. *arXiv preprint arXiv:1610.02024*.
- Liao H, et al. (2016) Gapless spin-liquid ground state in the $s = 1/2$ kagome antiferromagnet. *arXiv preprint arXiv:1610.04727*.
- Shimizu Y, Miyagawa K, Kanoda K, Maesato M, Saito G (2003) Spin liquid state in an organic mott insulator with a triangular lattice. *Phys. Rev. Lett.* 91(10):107001.
- Kurosaki Y, Shimizu Y, Miyagawa K, Kanoda K, Saito G (2005) Mott transition from a spin liquid to a fermi liquid in the spin-frustrated organic conductor $\kappa-(\text{ET})_2\text{Cu}_2(\text{CN})_3$. *Phys. Rev. Lett.* 95(17):177001.
- Itou T, Oyamada A, Maegawa S, Tamura M, Kato R (2007) Spin-liquid state in an organic spin-1/2 system on a triangular lattice. *etm 3 [npj(dmit) 2] 2. Journal of Physics: Condensed Matter* 19(14):145247.
- Itou T, Oyamada A, Maegawa S, Tamura M, Kato R (2008) Quantum spin liquid in the spin-1/2 triangular antiferromagnet $\text{Et}_3\text{me}_3\text{Sb}[\text{Pd}(\text{dmit})_2]_2$. *Phys. Rev. B* 77(10):104413.
- Isono T, et al. (2014) Gapless quantum spin liquid in an organic spin-1/2 triangular-lattice $\kappa - \text{h}_3(\text{cat-edt-tf})_2$. *Phys. Rev. Lett.* 112(17):177201.
- Yamada MG, Fujita H, Oshikawa M (2017) Designing katev spin liquids in metal-organic frameworks. *Phys. Rev. Lett.* 119(5):057202.
- Liu Z, Wang ZF, Mei JW, Wu YS, Liu F (2013) Flat chern band in a two-dimensional organometallic framework. *Phys. Rev. Lett.* 110(10):106804.
- Wu C, Bergman D, Balents L, Das Sarma S (2007) Flat bands and wigner crystallization in the honeycomb optical lattice. *Phys. Rev. Lett.* 99(7):070401.
- Wu C, Das Sarma S (2008) p_x, p_y -orbital counterpart of graphene: Cold atoms in the honeycomb optical lattice. *Phys. Rev. B* 77(23):235107.
- Tang E, Mei JW, Wen XG (2011) High-temperature fractional quantum hall states. *Phys. Rev. Lett.* 106(23):236802.
- Sun K, Gu Z, Katsura H, Das Sarma S (2011) Nearly flatbands with nontrivial topology. *Phys. Rev. Lett.* 106(23):236803.
- Neupert T, Santos L, Chamon C, Mudry C (2011) Fractional quantum hall states at zero magnetic field. *Phys. Rev. Lett.* 106(23):236804.
- Li W, Liu Z, Wu YS, Chen Y (2014) Exotic fractional topological states in a two-dimensional organometallic material. *Phys. Rev. B* 89(12):125411.
- Lahiri N, Lotfizadeh N, Tsuchikawa R, Deshpande VV, Louie J (2017) Hexaaminobenzene as a building block for a family of 2d coordination polymers. *Journal of the American Chemical Society* 139(1):19–22.
- Norman MR (2016) *Colloquium*: Herbertsmithite and the search for the quantum spin liquid. *Rev. Mod. Phys.* 88(4):041002.
- Lee PA, Nagaosa N, Wen XG (2006) Doping a mott insulator: Physics of high-temperature superconductivity. *Rev. Mod. Phys.* 78(1):17–85.
- Bartels L (2010) Tailoring molecular layers at metal surfaces. *Nat Chem* 2(2):87–95.
- Liu J, et al. (2011) Structural transformation of two-dimensional metal-organic coordination networks driven by intrinsic in-plane compression. *Journal of the American Chemical Society* 133(46):18760–18766. PMID: 21985163.
- Lin N, et al. (2007) Template-directed supramolecular self-assembly of coordination dumbbells at surfaces. *Chem. Commun.* (46):4860–4862.
- Pawin G, et al. (2008) A surface coordination network based on substrate-derived metal adatoms with local charge excess. *Angewandte Chemie International Edition* 47(44):8442–8445.
- Tait SL, et al. (2008) Assembling isostructural metal-organic coordination architectures on $\text{Cu}(100)$, $\text{Ag}(100)$ and $\text{Ag}(111)$ substrates. *ChemPhysChem* 9(17):2495–2499.
- Kamihara Y, Watanabe T, Hirano M, Hosono H (2008) Iron-based layered superconductor $\text{La}[\text{o}1\text{-x}]\text{Feas}$ ($x = 0.05\text{-}0.12$) with $T_c = 26$ K. *Journal of the American Chemical Society* 130(11):3296–3297.
- Dai J, Si Q, Zhu JX, Abrahams E (2009) Iron pnictides as a new setting for quantum criticality. *Proceedings of the National Academy of Sciences* 106(11):4118–4121.
- Kou SP, Li T, Weng ZY (2009) Coexistence of itinerant electrons and local moments in iron-based superconductors. *EPL (Europhysics Letters)* 88(1):17010.
- von Helmolt R, Wecker J, Holzapfel B, Schultz L, Samwer K (1993) Giant negative magnetoresistance in perovskitelike $\text{La}_{2/3}\text{Ba}_{1/3}\text{MnO}_x$ ferromagnetic films. *Phys. Rev. Lett.* 71(14):2331–2333.
- Ramirez AP (1997) Colossal magnetoresistance. *Journal of Physics: Condensed Matter*

- 9(39):8171.
45. Kondo J (1964) Resistance minimum in dilute magnetic alloys. *Progress of Theoretical Physics* 32(1):37–49.
 46. Anderson PW (1961) Localized magnetic states in metals. *Phys. Rev.* 124(1):41–53.
 47. Andres K, Graebner JE, Ott HR (1975) 4f-virtual-bound-state formation in CeAl₃ at low temperature. *Phys. Rev. Lett.* 35(26):1779–1782.
 48. Senthil T, Vojta M, Sachdev S (2004) Weak magnetism and non-fermi liquids near heavy-fermion critical points. *Phys. Rev. B* 69(3):035111.
 49. Bednorz JG, Müller KA (1986) Possible high T_c superconductivity in the Ba-La-Cu-O system. *Zeitschrift für Physik B Condensed Matter* 64(2):189–193.
 50. Mei JW, Kawasaki S, Zheng GQ, Weng ZY, Wen XG (2012) Luttinger-volume violating fermi liquid in the pseudogap phase of the cuprate superconductors. *Phys. Rev. B* 85(13):134519.
 51. White SR (1992) Density matrix formulation for quantum renormalization groups. *Phys. Rev. Lett.* 69(19):2863–2866.
 52. Kambe T, et al. (2013) π -conjugated nickel bis(dithiolene) complex nanosheet. *Journal of the American Chemical Society* 135(7):2462–2465.
 53. Kambe T, et al. (2014) Redox control and high conductivity of nickel bis(dithiolene) complex π -nanosheet: A potential organic two-dimensional topological insulator. *Journal of the American Chemical Society* 136(41):14357–14360.
 54. Senthil T, Sachdev S, Vojta M (2003) Fractionalized fermi liquids. *Phys. Rev. Lett.* 90(21):216403.
 55. Mielke A (1991) Ferromagnetic ground states for the hubbard model on line graphs. *Journal of Physics A: Mathematical and General* 24(2):L73.
 56. Mielke A (1991) Ferromagnetism in the hubbard model on line graphs and further considerations. *Journal of Physics A: Mathematical and General* 24(14):3311.

DRAFT